Model-Independent Constraints on Extra Neutral Gauge Bosons from the Process $e^-e^+ \rightarrow \mu^-\mu^+$

Elias Assmann

11th June 2007

Contents

Chapter 0

Introduction

0.1 About the LPSC

The *Laboratoire de Physique Subatomique et de Cosmologie* (LPSC) is an institute of fundamental research at the *Polygône Scientifique* of Grenoble. It represents a cooperation of the *Institut National de Physique Nucléaire et de Physique des Particules* (IN2P3), the *Université Joseph Fourier* (UJF) and the *Institut National Polytechnique de Grenoble* (INPG). It employs some 200 people and represents a major player in physics research at the national French level. In addition, it is involved in numerous scientific collaborations of worldwide scope.

The institute's major areas of study include the geometry, composition and evolution of the universe; unification of the fundamental forces; quantum chromodynamics and nucleon structure. It pursues both experimental and theoretical research.

This internship took place in the theory group of the LPSC. It is part of an ongoing project concerning the Z′.

0.2 About the Standard Model and the Z′

The Standard Model (SM) of particle physics has been immensely successful, in the sense that its predictions have been verified with unparalleled precision. Nevertheless, it is believed by many to be only an effective theory, valid at small energy scales[1]. While the SM is known to be incomplete (e.g. by neutrino oscillations [5]), this belief is motivated to a substantial part by aesthetic perceptions: the SM gauge group

$$\mathrm{SU}(3)_c \times \mathrm{SU}(2)_L \times \mathrm{U}(1)_Y, \tag{0.1}$$

---

[1] for some sufficiently large value of "small"

being composed of three independent factors, is perceived to be complicated, and one tries to replace it by some simple[2] gauge group ($SU(5)$ and $SO(10)$ are two examples of popular candidates). To be consistent with experiment and reproduce the SM successes, this unifying group has to contain SM gauge group as a subgroup, and has to be broken at some energy scale E_{GUT} to reproduce it.

Such a theory this is termed a *Grand Unification Theory*, or *GUT* for short, because the three fundamental forces of the SM are unified under one symmetry. A GUT is to the electroweak and strong interactions what electroweak theory is to the electromagnetic and weak interactions; or what quantum electrodynamics, in turn, is to electricity and magnetism. On the other hand, a theory which would unify a GUT with gravity, is quite appropriately referred to as a *TOE* (*Theory Of Everything*), as it would unify all four known fundamental forces.

In the process of breaking the GUT symmetry, very often additional $U(1)$ factors appear. These factors imply an additional neutral gauge boson which is generically called Z' in analogy to the SM Z. Such bosons have to be either very heavy or very weakly coupled so as not to break the success of the SM.

0.3   About this Study

In this study, we consider the case where the SM is extended by one extra neutral gauge boson Z' with mass $M_{\mathrm{Z'}}$ and couplings to the SM fermions of the form

$$-\mathrm{i}\,\gamma^{\alpha} g_{\mathrm{Z'}} \left(v_{\mathrm{Z'}}^{f} - a_{\mathrm{Z'}}^{f} \right)$$

(cf. Section 1.1). This extension must of course reproduce the excellent agreement of the SM with experimental results. Qualitatively, it seems clear that this will imply stringent constraints on the parameter space of the Z'.

This study is an attempt to give quantitative meaning to this statement, and to do so in a manner largely independent of any particular model. We must however make some assumptions to reduce this task to manageable proportions.

Throughout the numerical analysis (Chapter 2), we have assumed $B - L$ coupling of the Z' to all SM fermions. That is, the charge of a fermion with respect to the new boson is $\frac{1}{3}$ for quarks and -1 for leptons; there are no chargeless SM fermions and the interaction is generation-independent. Furthermore, we assume only vectorial and no axial coupling. This assumption is only a convenience. It allows us to operate in a two-dimensional parameter space, making visualization of the results that much easier. It would not be difficult to modify the analysis to include axial couplings.

In the terms introduced in Chapter 1:

---

[2]In the group theoretical and, by extension, in the aesthetic sense

$$v_{Z'}^{f} = B_f - L_f \quad \text{for all SM fermions } f,$$
$$v_{Z'}^{X} = 0 \qquad \text{for all other } X; \tag{0.2}$$
$$a_{Z'}^{X} = 0 \qquad \text{for all } X.$$

A $U(1)_{B-L}$ factor is a realistic possibillity appearing in many extensions of the SM. It implies a Z' with coupling strengths proportional to $B - L$ as well as making $B - L$ a conserved quantity.

In the SM, both B and L individually are approximately conserved and $B - L$ conservation is even stronger: in all SM processes that violate B or L conservation, these contributions cancel and $B - L$ remains conserved.

Finally, there is a simple phenomenological reason to this choice: $B - L$ charge can be probed by *any* experiment, for quarks and leptons will always intervene. By contrast, some models postulate a Z' that couples only to third generation fermions to avoid constraints from low-energy data.

As for the rest of this report, Chapter 1 of this report contains the analytical calculation of $\sigma(e^-e^+ \to \gamma, Z, Z' \to f\bar{f})$ and $\Gamma_{Z'}$. These calculations have been kept quite general. Specifically, they are independent of any particular charge scheme, in contrast to the numerical analysis.

In Chapter 2, we exploit the formulae found in Chapter 1 for a numerical analysis using data on the process $e^-e^+ \to \mu^-\mu^+$ from the colliders PETRA at DESY, TRISTAN at KEK and LEP at CERN.[3] Our assumption about the fermion charges relative to the extra boson leaves us with just two parameters for the latter: the mass $M_{Z'}$ and the coupling strength $g_{Z'}$. Using χ^2 statistics, we trace an exclusion plot in the $(M_{Z'}, g_{Z'})$ plane.

Finally, in Chapter 3, we discuss some limitations of this study and give a short outlook towards possible extensions.

---

[3]For reference, the data is compiled in App. A.

Chapter 1

Analytic Calculations

1.1 Feynman Rules

We consider the reaction $e^- e^+ \to f\overline{f}$, mediated by a vector boson B.[1] Spin and momentum names are defined in Fig. 1.1. First, recall the Feynman rules from electroweak theory compiled in Table 1.1 (taken from [6]).

The weak charges in the SM are

$$c_V^f = T_f^3 - 2Q_f \sin^2\theta_W, \tag{1.1}$$

$$c_A^f = T_f^3 \tag{1.2}$$

where θ_W is the Weinberg angle, $\sin^2\theta_W = 0.23$. The values are collected in Table 1.2.

Next, let us introduce "generic" rules, that shall depend on B and apply to all bosons we consider. They are

$$-i\ V_B^{f\,\alpha} := -i\ \gamma^\alpha g_B \left(v_B^f - a_B^f \gamma^5\right) \tag{1.3}$$

for the $f\overline{f}B$ vertex and

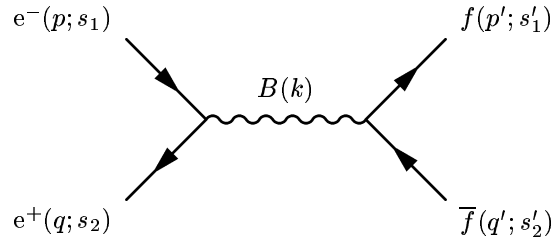[1] In fact, we work under the assumption $f \neq e$; otherwise, a second diagram contributes.

Figure 1.1: Four-momenta and spins as used in the calculations below.

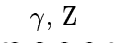Table 1.1: Feynman rules for $-\mathrm{i}\,\mathfrak{M}$ for electroweak processes

External lines (in, out)

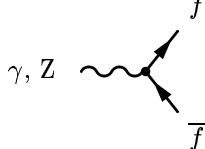|		
Spin $\frac{1}{2}$ (anti)fermion		$u, \bar{u} \quad (v, \bar{v})$
Spin 1 boson		$\varepsilon_\alpha, \varepsilon_\alpha^*$

γ propagator $\qquad\qquad \gamma, Z \qquad\qquad -\mathrm{i}\, g_{\alpha\beta}/k^2$

Z propagator $\qquad$ $\qquad -\mathrm{i}\, \dfrac{g_{\alpha\beta} - k_\alpha k_\beta/M_Z^2}{k^2 - M_Z^2 + \mathrm{i}\, M_Z \Gamma_Z}$

γ vertex $\qquad\qquad\qquad\qquad\qquad -\mathrm{i}\, Q^f \gamma^\alpha$

γ, Z

Z vertex $\qquad\qquad\qquad\qquad\qquad -\mathrm{i}\, \dfrac{e}{2\sin\theta_\mathrm{W}\cos\theta_\mathrm{W}} \gamma^\alpha \left(c_\mathrm{V}^f - c_\mathrm{A}^f \gamma^5 \right)$

Table 1.2: Weak charges in the SM ($s^2 := \sin^2\theta_\mathrm{W}$)

	u, c, t	d, s, b	$\nu_\mathrm{e}, \nu_\mu, \nu_\tau$	$\mathrm{e}^-, \mu^-, \tau$
c_V	$\frac{1}{2} - \frac{4}{3}s^2$	$-\frac{1}{2} + \frac{2}{3}s^2$	$\frac{1}{2}$	$-\frac{1}{2} + 2s^2$
c_A	$\frac{1}{2}$	$-\frac{1}{2}$	$\frac{1}{2}$	$-\frac{1}{2}$

$$-\mathrm{i}\,\chi_B(k)\,T_{B\,\alpha\beta}(k) := -\mathrm{i}\,\frac{1}{k^2 - M_B^2 + \mathrm{i}\, M_B \Gamma_B}\left(g_{\alpha\beta} - \tilde{M}_B^2 k_\alpha k_\beta\right) \qquad (1.4)$$

for the B propagator, letting $\tilde{M}_\gamma^2 = 0$ for the photon and $\tilde{M}_B^2 = 1/M_B^2$ for a massive boson B.

Comparing (1.3) with Table 1.1, we can make the following identifications for the photon and the Z boson:

$$g_\gamma = e, \qquad\qquad v_\gamma^f = Q^f/e, \qquad a_\gamma^f = 0; \qquad (1.5)$$

$$g_\mathrm{Z} = \frac{e}{2\sin\theta_\mathrm{W}\cos\theta_\mathrm{W}}, \qquad v_\mathrm{Z}^f = c_\mathrm{V}^f, \qquad a_\mathrm{Z}^f = c_\mathrm{A}^f. \qquad (1.6)$$

In the next section, we will calculate the matrix element of the Feynman diagram Fig. 1.1, in terms of these Feynman rules. This will allow us to find the result for any specific case (i.e a fermion/boson combination) by filling in the variables depending on f and B.

1.2 The Matrix Element of $\mathrm{e}^-\mathrm{e}^+ \to f\overline{f}$

The matrix element corresponding to Fig. 1.1 is

$$
-\mathrm{i}\,\mathfrak{M}_B = \bar{v}_\mathrm{e}(q;s_2)\left[-\mathrm{i}\,V_B^{\mathrm{e}\,\alpha}\right]u_\mathrm{e}(p;s_1)\chi_B(k)\left[-\mathrm{i}\,T_{B\,\alpha\beta}(k)\right]\cdot
$$
$$
\cdot\,\bar{u}_f(p';s_1')\left[-\mathrm{i}\,V_B^{f\,\beta}\right]v_f(q';s_2'). \quad (1.7)
$$

Any physical quantity will depend only on the squared modulus of the matrix element, to wit

$$
|\mathfrak{M}|^2 = \left|\sum_B \mathfrak{M}_B\right|^2 = \sum_{B\,B'} \mathfrak{M}_B\,\mathfrak{M}_{B'}^*.
$$

We therefore compute a general expression of $\mathfrak{M}_B\,\mathfrak{M}_{B'}^*$. The complex conjugate of the matrix element is

$$
\mathfrak{M}_B^* = \bar{v}_f(q';s_2')V_B^{f\,\sigma}u_f(p';s_1')\chi_B^* T_{B\,\rho\sigma}\bar{u}_\mathrm{e}(p;s_1)V_B^{\mathrm{e}\,\rho}v_\mathrm{e}(q;s_2). \quad (1.8)
$$

Additionally, we must take into account particle spins and colors. As a general rule (in absence of polarization), one has to average over all spin and color states of the incident particles and sum over those of the outgoing particles. We therefore need

$$
\overline{\mathfrak{M}_B\,\mathfrak{M}_{B'}^*} = \frac{1}{2s_{\mathrm{e}^-}+1}\frac{1}{2s_{\mathrm{e}^+}+1}\sum_{\substack{\text{spin/color}\\\text{states}}}\mathfrak{M}_B\,\mathfrak{M}_{B'}^*
$$
$$
= N_\mathrm{c}^f\frac{1}{4}\sum_{s_1,\ldots,s_2'}\bar{v}_\mathrm{e}(q;s_2)V_B^{\mathrm{e}\,\alpha}u_\mathrm{e}(p;s_1)\chi_B T_{B\,\alpha\beta}\bar{u}_f(p';s_1')V_B^{f\,\beta}v_f(q';s_2')
$$
$$
\cdot\,\bar{v}_f(q';s_2')V_{B'}^{f\,\sigma}u_f(p';s_1')\chi_{B'}^* T_{B'\,\rho\sigma}\bar{u}_\mathrm{e}(p;s_1)V_{B'}^{\mathrm{e}\,\rho}v_\mathrm{e}(q;s_2).
$$

Rearranging by spins:

$$
\overline{\mathfrak{M}_B\,\mathfrak{M}_{B'}^*} = N_\mathrm{c}^f\,\chi_B\chi_{B'}^*\frac{1}{2}\sum_{s_1,s_2}\bar{v}_\mathrm{e}(q;s_2)V_B^{\mathrm{e}\,\alpha}u_\mathrm{e}(p;s_1)\bar{u}_\mathrm{e}(p;s_1)V_{B'}^{\mathrm{e}\,\rho}v_\mathrm{e}(q;s_2)
$$
$$
\cdot\,T_{B\,\alpha\beta}T_{B'\,\rho\sigma}\frac{1}{2}\sum_{s_1',s_2'}\bar{u}_f(p';s_1')V_B^{f\,\beta}v_f(q';s_2')\bar{v}_f(q';s_2')V_{B'}^{f\,\sigma}u_f(p';s_1')
$$
$$
=: N_\mathrm{c}^f\,\chi_B\chi_{B'}^*\,L_{BB'}{}^{\alpha\rho}T_{B\,\alpha\beta}T_{B'\,\rho\sigma}L_{BB'}'{}^{\beta\sigma}
$$
$$
(1.9)
$$

where we have introduced the fermion tensors

$$L_{BB'}{}^{\alpha\rho} = \frac{1}{2}\sum_{s_1,s_2}\bar{v}_{\rm e}(q;s_2)V_B^{{\rm e}\,\alpha}u_{\rm e}(p;s_1)\bar{u}_{\rm e}(p;s_1)V_{B'}^{{\rm e}\,\rho}v_{\rm e}(q;s_2),$$

$$L'_{BB'}{}^{\beta\sigma} = \frac{1}{2}\sum_{s'_1,s'_2}\bar{u}_f(p';s'_1)V_B^{f\,\beta}v_f(q';s'_2)\bar{v}_f(q';s'_2)V_{B'}^{f\,\sigma}u_f(p';s'_1) \qquad (1.10)$$

$$= L_{B'B}{}^{\sigma\beta}\Big|_{\substack{p\to p'\\ q\to q'\\ {\rm e}\leftrightarrow f}}$$

and $N_{\rm c}^f$ is the number of color states of the outgoing fermion f i.e. $N_{\rm c}^q = 3; N_{\rm c}^\ell = 1$.

As $L_{BB'}{}^{\alpha\rho}$ is a scalar[2], we can view it as its own trace; this allows us to use the cyclic property of the trace to separate the intervening wave functions. That is, we can write

$$L_{BB'}{}^{\alpha\rho} = \frac{1}{2}\,{\rm Tr}\left\{\sum_{s_2}v_{\rm e}(q;s_2)\bar{v}_{\rm e}(q;s_2)V_B^{{\rm e}\,\alpha}\sum_{s_1}u_{\rm e}(p;s_1)\bar{u}_{\rm e}(p;s_1)V_{B'}^{{\rm e}\,\rho}\right\}. \quad (1.11)$$

Finally, using the completeness relations

$$\sum_s u(k;s)\bar{u}(k;s) = \slashed{k} + m, \qquad\qquad \sum_s v(k;s)\bar{v}(k;s) = \slashed{k} - m$$

we find

$$L_{BB'}{}^{\alpha\rho} = \frac{1}{2}\,{\rm Tr}\left\{(\slashed{q} - m_{\rm e})V_B^{{\rm e}\,\alpha}(\slashed{p} + m_{\rm e})V_{B'}^{{\rm e}\,\rho}\right\},$$

$$L'_{BB'}{}^{\beta\sigma} = \frac{1}{2}\,{\rm Tr}\left\{(\slashed{p}' + m_f)V_B^{f\,\beta}(\slashed{q}' - m_f)V_{B'}^{f\,\sigma}\right\}. \qquad (1.12)$$

To complete the calculation, some kinematics is in order. We use the relativistically invariant Mandelstam variables s, t and u as defined in Fig. 1.2 and neglect the fermion masses (a valid approximation for all the data used in this analysis).

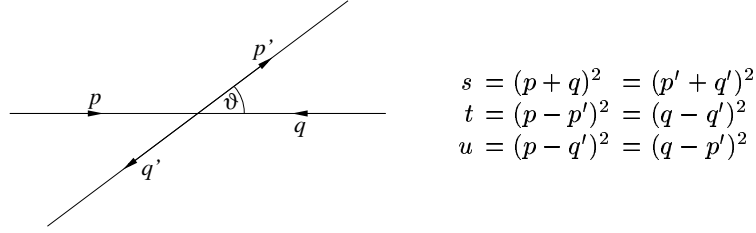The Mandelstam variables are not independent but are linked by

$$s + t + u = \sum_i m_i^2 = 2m_{\rm e}^2 + 2m_f^2 \approx 0. \qquad (1.13)$$

We use this to eliminate u, and furthermore replace t with the scattering angle ϑ (taken in the center-of-mass frame). Again in the ultra-relativistic limit, we have

---

[2]With respect to Dirac indices but not in the sense of a Lorentz scalar.

$$s = (p + q)^2 = (p' + q')^2$$
$$t = (p - p')^2 = (q - q')^2$$
$$u = (p - q')^2 = (q - p')^2$$

Figure 1.2: Kinetics of $e^- e^+ \to f\overline{f}$.

$$t = -s(1 - \cos\vartheta)/2. \tag{1.14}$$

Taken together, this leads to the relations

$$
\begin{aligned}
q \cdot p &= p' \cdot q' = & s/2, \\
p \cdot p' &= q' \cdot q = & -t/2 = s(1 - \cos\vartheta)/4, \\
p \cdot q' &= p' \cdot q = & (s + t)/2 = s(1 + \cos\vartheta)/4.
\end{aligned}
\tag{1.15}
$$

We need now but apply (1.15) and the trace theorems for the γ matrices to find the desired result. Straightforward but tedious calculation[3] yields

$$\overline{\mathfrak{M}_B \mathfrak{M}_{B'}^*} = N_c^f s^2 \chi_B \chi_{B'}^* g_B^2 g_{B'}^2 \left[2\, C_{BB'}^{ef} \cos\vartheta + D_{BB'}^{ef} \left(1 + \cos^2\vartheta \right) \right] \tag{1.16}$$

with

$$C_{BB'}^{ef} = v_B^e v_B^f a_{B'}^e a_{B'}^f + v_B^e a_B^f a_{B'}^e v_{B'}^f + a_B^e v_B^f v_{B'}^e a_{B'}^f + a_B^e a_B^f v_{B'}^e v_{B'}^f, \tag{1.17}$$

$$D_{BB'}^{ef} = v_B^e v_B^f v_{B'}^e v_{B'}^f + v_B^e a_B^f v_{B'}^e a_{B'}^f + a_B^e v_B^f a_{B'}^e v_{B'}^f + a_B^e a_B^f a_{B'}^e a_{B'}^f. \tag{1.18}$$

summarizing the dependence of $\overline{\mathfrak{M}_B \mathfrak{M}_{B'}^*}$ on the fermion charges.

Note that both C and D are symmetric under both of the exchanges $e \leftrightarrow f$ and $B \leftrightarrow B'$.

1.3 The Cross Section of $e^- e^+ \to f\overline{f}$

1.3.1 The Differential Cross Section

The angular differential cross section of the process $e^- e^+ \to f\overline{f}$ in the center-of-mass frame is

$$\frac{d\sigma}{d\Omega} = \frac{1}{64\pi^2 s} \overline{\left| \sum_B \mathfrak{M}_B \right|^2} = \sum_{BB'} \frac{1}{64\pi^2 s} \overline{\mathfrak{M}_B \mathfrak{M}_{B'}^*} =: \sum_{BB'} \frac{d\sigma_{BB'}}{d\Omega} \tag{1.19}$$

---

[3]Most easily carried out with *Mathematica* and and the package *Tracer* [8] — see App. B.

where we have identified a contribution $\mathrm{d}\sigma_{BB'}/\mathrm{d}\Omega$ with each combination (B, B') of vector bosons that can mediate the reaction. In the case of $B = B'$, this result is real (in the mathematical sense) and physical; for the interference terms $B \neq B'$, only the sum $\mathrm{d}(\sigma_{B,B'} + \sigma_{B',B})/\mathrm{d}\Omega$ is.

This contribution factorizes into two parts, one depending only on s and one only on ϑ:

$$\frac{\mathrm{d}\sigma_{BB'}}{\mathrm{d}\Omega} =: \frac{1}{64\pi^2} F_{BB'}(s) G_{BB'}^{\mathrm{ef}}(\cos\vartheta) \tag{1.20}$$

with

$$F_{BB'}(s) = s\chi_B \chi_{B'}^* = \frac{s}{\left(s - M_B^2 + \mathrm{i}\,M_B\Gamma_B\right)\left(s - M_{B'}^2 - \mathrm{i}\,M_{B'}\Gamma_{B'}\right)} \tag{1.21}$$

and

$$G_{BB'}^{\mathrm{ef}}(\cos\vartheta) = N_{\mathrm{c}}^f\, g_B^2 g_{B'}^2 \left[2\, C_{BB'}^{\mathrm{ef}} \cos\vartheta + D_{BB'}^{\mathrm{ef}}(1 + \cos^2\vartheta)\right]. \tag{1.22}$$

1.3.2 The Integrated Cross Section

Thanks to the simple structure of the decomposition (1.20), the angular integration becomes very simple:

$$\begin{aligned}
\sigma_{\mathrm{tot}}(s) &= \sum_{BB'} \int \mathrm{d}\Omega\, \frac{\mathrm{d}\sigma_{BB'}}{\mathrm{d}\Omega} \\
&= \sum_{BB'} \frac{1}{64\pi^2} F_{BB'}(s)\, 2\pi \int_{-1}^{+1} \mathrm{d}(\cos\vartheta)\, G_{BB'}^{\mathrm{ef}}(\cos\vartheta) \\
&= \sum_{BB'} \frac{1}{12\pi} F_{BB'}(s) D_{BB'}^{\mathrm{ef}}.
\end{aligned} \tag{1.23}$$

1.3.3 Adaptations for Numerical Study

To avoid dealing with complex numbers in the numerical study, we substitute

$$\begin{aligned}
F_{BB'}(s) &\to \mathrm{Re}\,F_{BB'}(s) = \\
&\frac{(s - M_B^2)(s - M_{B'}^2) + M_B\Gamma_B M_{B'}\Gamma_{B'}}{\left[(s - M_B^2)^2 + (M_B\Gamma_B)^2\right]\left[(s - M_{B'}^2)^2 + (M_{B'}\Gamma_{B'})^2\right]}
\end{aligned} \tag{1.24}$$

which of course cancels leaves the sum $F_{BB'} + F_{B'B} = 2\,\mathrm{Re}\,F_{BB'} = 2\,\mathrm{Re}\,F_{B'B}$ unchanged.
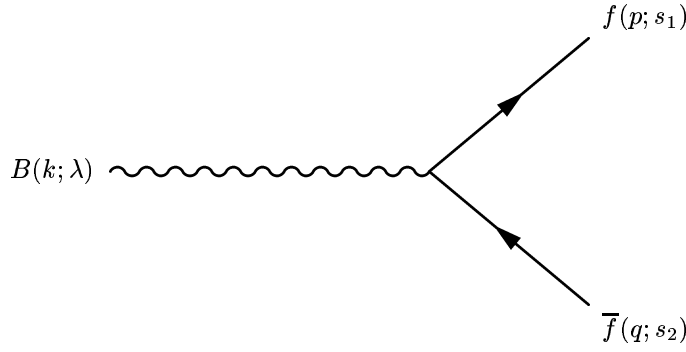
Figure 1.3: Decay of a boson B (four-momentum k, helicity λ) into a fermion pair $f\overline{f}$

Furthermore, to properly reproduce experimental results, it may be necessary to introduce "cuts" in the integrated cross section to account for the geometry of the detector and for the experimental analysis. The integral in (1.23) then becomes

$$\int_{-1}^{+1} \mathrm{d}(\cos\vartheta)\,\Theta_{\mathrm{exp}}(\cos\vartheta)G_{BB'}(\cos\vartheta) \tag{1.25}$$

with a suitable indicator function Θ_{exp}.

1.4   The Decay Width of a Massive Neutral Gauge Boson

We consider decays of a neutral massive gauge boson into fermion pairs. Each such decay mode $B \to f\overline{f}$ contributes a partial width to the total width Γ_B. The partial width is (in the Born approximation)

$$\begin{aligned}
\Gamma(B \to f\overline{f}) &= \frac{p_{\mathrm{f}}}{32\pi^2 M_B^2} \int \mathrm{d}\Omega\, \overline{\left|\mathfrak{M}(B \to f\overline{f})\right|^2} \\
&= \frac{p_{\mathrm{f}}}{8\pi M_B^2} \overline{\left|\mathfrak{M}(B \to f\overline{f})\right|^2}
\end{aligned} \tag{1.26}$$

where $p_{\mathrm{f}} = \|\vec{p}_f\| = \|\vec{p}_{\overline{f}}\|$ is the norm of the three-momentum in the final state, taken in the center-of-mass frame; and $\mathfrak{M}(B \to f\overline{f})$ is the matrix element of the decay (i.e. of the Feynman graph Fig. 1.3).

p_{f} is easily calculated via the Mandelstam variable

$$s = M_B^2 = \left(E_f + E_{\overline{f}},\ \vec{p}_f + \vec{p}_{\overline{f}}\right)^2 = \left(2\sqrt{m_f^2 + p_{\mathrm{f}}^2}\right)^2$$

such that

$$p_{\mathrm{f}} = \sqrt{M_B^2/4 - m_f^2} = \frac{M_B}{2}\sqrt{1 - 4r_f^2} \tag{1.27}$$

with $r_f := m_f/M_B$.

Note that it is no longer justified to neglect the fermion masses because we wish to be able to calculate the width for any given boson mass.

The matrix element is

$$
\begin{aligned}
\mathfrak{M}_f &= \varepsilon_\alpha(k;\lambda)\bar{u}(p;s_1)V_B^{f\,\alpha}v(q;s_2),\\
\mathfrak{M}_f^* &= \varepsilon_\beta^*(k;\lambda)\bar{v}(q;s_2)V_B^{f\,\beta}u(p;s_2).
\end{aligned}
\tag{1.28}
$$

Again, we need the modulus squared, averaged over incoming (boson) and summed over outgoing (fermion) spin and color configurations.

$$
\begin{aligned}
\overline{\left|\mathfrak{M}_f\right|^2} &= \frac{N_{\mathrm{c}}^f}{2s_B+1}\sum_\lambda \varepsilon_\alpha(k;\lambda)\varepsilon_\beta(k;\lambda)\\
&\quad \cdot \operatorname{Tr}\left\{\sum_{s_1} u(p;s_1)\bar{u}(p;s_1)V_B^{f\,\alpha}\sum_{s_2} v(q;s_2)\bar{v}(q;s_2)V_B^{f\,\beta}\right\}\\
&= \frac{1}{3}\left(\frac{k_\alpha k_\beta}{M_B^2} - g_{\alpha\beta}\right)\operatorname{Tr}\left\{(\slashed{q}-m)V_B{}^{f\alpha}(\slashed{p}+m)V_B^{f\,\beta}\right\}
\end{aligned}
\tag{1.29}
$$

using the same method that led to (1.11). Note that this result is of the form $-\frac{2}{3}T_{\alpha\beta}L^{\alpha\beta}$.

Applying the γ trace theorems, we find

$$\overline{\left|\mathfrak{M}_f\right|^2} = \frac{4}{3}N_{\mathrm{c}}^f g_B^2 M_B^2\left[\left(1+2r_f^2\right)v_B^{f\,2} + \left(1-4r_f^2\right)a_B^{f\,2}\right] \tag{1.30}$$

for the matrix element and

$$\Gamma(B \to f\overline{f}) = \frac{1}{12\pi}N_{\mathrm{c}}^f g_B^2 M_B\sqrt{1-4r_f^2}\left[\left(1+2r_f^2\right)v_B^{f\,2} + \left(1-4r_f^2\right)a_B^{f\,2}\right] \tag{1.31}$$

for the partial width.

To give an idea of the accuracy of this formula, take the SM Z; our method gives $\Gamma_{\mathrm{Z}} = 2.2760$ GeV, compared to the published value of $\Gamma_{\mathrm{Z}} = 2.4952 \pm 0.0023$ GeV [10]. This is satisfactory for our analysis, whose sensitivity to Γ is limited. Note, however, that somewhat larger errors are to be expected near the quark masses, due to non-perturbative QCD effects.

Chapter 2

Numerical Analysis

In this chapter, we will apply the results from Chapter 1 to produce an exclusion plot in the $(M_{Z'}, g_{Z'})$ plane. The data we have used is compiled in Table A.1. Fig. A.1 shows a comparison of the data to the theoretical cross section as calculated in (1.23).

As discussed in Section 0.3, we assume for this analysis that exactly one extra neutral gauge boson contributes to the cross section. That is, we consider the reaction

$$e^- e^+ \to \gamma, Z, Z' \to \mu^- \mu^+. \tag{2.1}$$

Furthermore, we assume coupling to all SM fermions according to (1.3) and (0.2).

The decay width $\Gamma_{Z'}$ of the boson enters the analysis through (1.4) and ends up in the cross section (1.23) via $F_{BB'}$ as defined in (1.21) (or rather (1.24)). We use (1.31) to compute $\Gamma_{Z'}$, considering decay into all SM quarks and leptons[1]. The fermion masses used for this calculation are reported in Table 2.1. The lepton and π meson masses are from [10]. For c, t, b we have chosen masses as they are typically used in the literature. We have assumed massless neutrinos. Given the energy range of the input data, this study is not very sensitive to the quark masses.

---

[1] The constraint $M_{Z'} \geq 2m_f$ is enforced, even though it does not explicitly figure in (1.31).

Table 2.1: Fermion masses as used in the calculation of the Z' decay width

	m_ℓ		m_q		m_q
e	511 keV	u	135 MeV $(= m_{\pi^0})$	d	135 MeV $(= m_{\pi^0})$
μ	106 MeV	c	1.5 GeV	s	498 MeV $(= m_{K^0})$
τ	1.78 GeV	t	175 GeV	b	4.5 GeV

2.1 χ^2 Statistics

We use χ^2 statistics to decide whether a given point $(M_{\mathrm{Z}'}, g_{\mathrm{Z}'})$ can be excluded.

Let y be a physical quantity, and $f(x \mid \mathcal{P})$ a model which predicts the value of y as a function of some other quantity x with parameters $\mathcal{P}$. The quantity y is measured at N different points x_i; let the results of the measurement be y_i with uncertainties of Δy_i.

The χ^2 statistic is then defined as

$$\chi^2_{\mathcal{P}} := \sum_{i=1}^{N} \left(\frac{y_i - f(x_i \mid \mathcal{P})}{\Delta y_i} \right)^2 . \tag{2.2}$$

Provided the the model is correct and the measured data are individually normally distributed with means y_i and variances $(\Delta y_i)^2$, this statistic will in fact follow a χ^2 distribution with N degrees of freedom.

In this case, one expects a value of $\chi^2/N \approx 1$, since each datum should be, on average, at one standard deviation from its expectation value. For the data in Table A.1, we find

$$\chi^2_{\mathrm{SM}}/N = 1.028 \qquad \text{with } N = 44 \tag{2.3}$$

with the "model"

$$\sigma(s \mid \mathrm{SM}) = \begin{cases} \sigma_{\mathrm{SM}} & \text{from Table A.1 if given} \\ \sigma_{\mathrm{tot}} & \text{from (1.23) otherwise} \end{cases}$$

See Chapter 3 for some discussion on σ_{SM} versus σ_{tot}. Note that σ_{SM} is only missing for the data from the TASSO experiment [4]; at those energies, higher-order corrections are negligible and the data are in good agreement with (1.23) (we refer to Fig. A.1 for qualitative justification of this statement).

We will regard a Z$'$ with parameters $(M_{\mathrm{Z}'}, g_{\mathrm{Z}'})$ as compatible with the data if

$$\Delta \chi^2_{(M_{\mathrm{Z}'}, g_{\mathrm{Z}'})} := \chi^2_{\mathrm{SM}+\mathrm{Z}'(M_{\mathrm{Z}'}, g_{\mathrm{Z}'})} - \chi^2_{\mathrm{SM}}$$
$$< \Delta \chi^2_{\mathrm{lim}} \tag{2.4}$$

where $\Delta \chi^2_{\mathrm{lim}}$ is a parameter which determines how safe our limit will be. In this study, we take a conservative point of view and require that

$$\Delta \chi^2_{(M_{\mathrm{Z}'}, g_{\mathrm{Z}'})}/N < 6. \tag{2.5}$$

Note that within the limits imposed by the accuracy of this study, the particular value of $\Delta \chi^2_{\mathrm{lim}}$ is not crucial as χ^2 rises very steeply with $g_{\mathrm{Z}'}$ (cf. Fig. 2.1 (b)).

Starting from these definitions, the exclusion plot Fig. 2.1 (a) is constructed by interval bisection until the relative error $\left| \Delta \chi^2 - \Delta \chi^2_{\mathrm{lim}} \right| / \Delta \chi^2_{\mathrm{lim}}$ is within a certain tolerance. (Specifically, the tolerance is 0.1% in Fig. 2.1 (a).)

2.2 Results and Figures

The results of the χ^2 analysis are represented in Fig. 2.1. At higher masses, the behavior remains qualitatively the same, until about 1800 GeV, where the significance of the data rapidly diminishes and we can no longer exclude anything. In Table 2.2, we give numerical limits for $g_{Z'}$ for some values of $M_{Z'}$. Like the graph of Fig. 2.1 (a), these were computed using $\Delta\chi^2_{\text{lim}} = 6$. Concerning the first value, there is a data point at exactly $M = 200$ GeV, therefore the graph spikes down to very small g there. The given value corresponds to a smoothed curve, disregarding the spike.
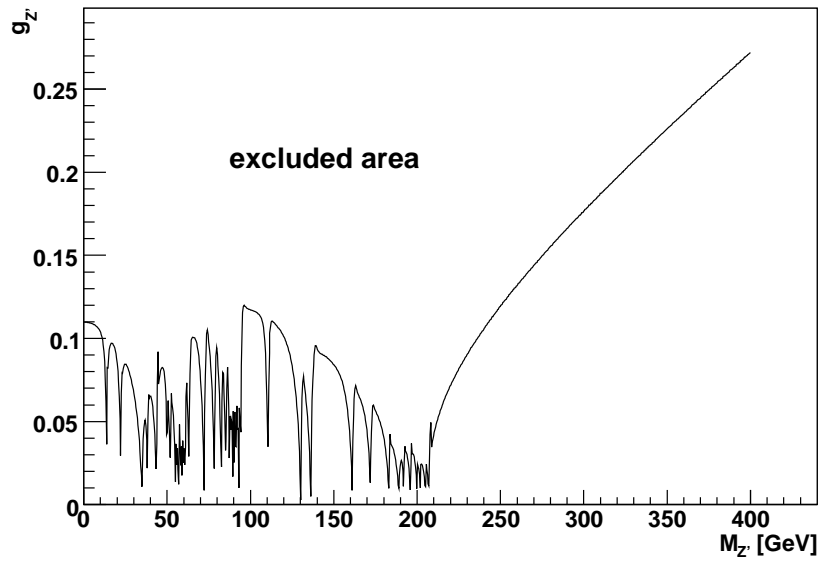
Fig. 2.2 shows a simulation of a Z' with $M_{Z'} = 200$ GeV and $g_{Z'} = g_Z/10 \approx 0.036$ (an excluded case, of course).

Finally, Fig. 2.3 shows an integration of our exclusion plot into an ongoing LPSC/ILL project [11]. We show this only to gain some perspective. It is beyond the scope of this report to enter into the details of the other lines.
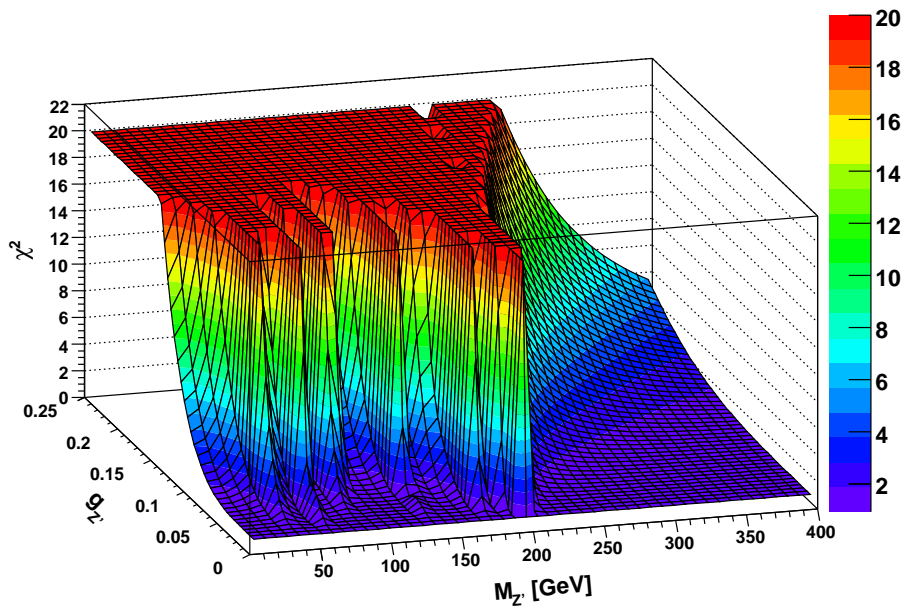
Table 2.2: Limits for $g_{Z'}$ for some values of $M_{Z'}$.

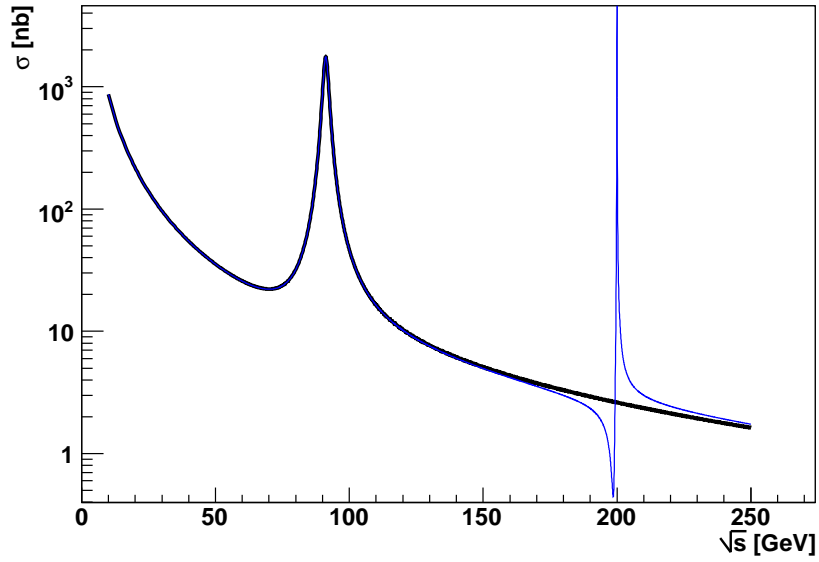| $M_{Z'}$ [GeV]	200	600	1000	1400	1800
$g_{Z'}^{\text{min}}$	0.026	0.45	0.77	1.1	1.7

(a)

(b)

Figure 2.1: Graphs resulting from the numerical analysis. (a) shows the limit $\Delta\chi^2 = 6$, (b) shows the relief of χ^2 over the (M, g) plane with a cutoff of $\chi^2 = 20$.

(a)
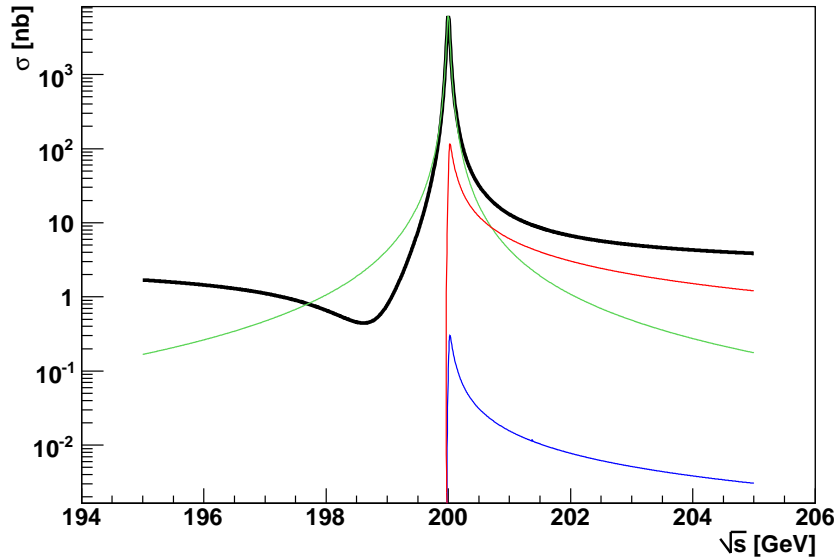
(b)

Figure 2.2: Simulation of a Z' with $M_{Z'} = 200\,\text{GeV}$ and $g_{Z'} = g_{Z}/10 \approx 0.036$. In (a), the black line shows the SM prediction (1.23) and the blue line shows the prediction for SM + Z'. In the zoom (b), the black line is SM + Z', the Z' Z' term is shown in green and the interferences in red (Z' γ) and blue (Z' Z).

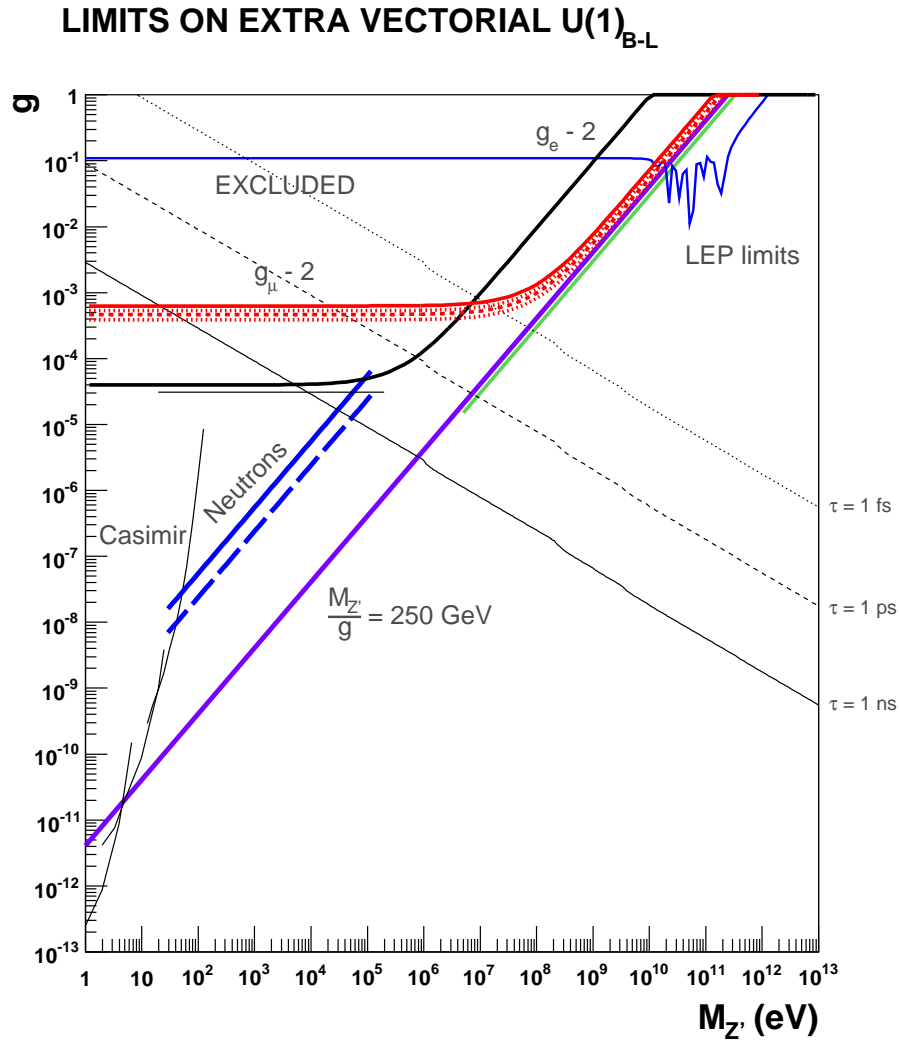Figure 2.3: Integration of the exclusion plot from this study into a larger one. Ours is the blue line labeled "LEP limits". The diagonal black lines also originated in this study. They show different Z′ lifetimes. This figure shows the complementarity of the present study to recent constraints on ultralight new bosons with ultra-cold neutrons.[11]

Chapter 3

Conclusion

It is clear that this study is far from complete. First of all, there is much additional data one could add. It would be straightforward to add more data on dimuon production, as well as to add tau or quark pair data. This can however not be expected to yield much new insight since the physics of those processes are ultimately not very different from dimuon production.

A more interesting perspective is therefore to add data on other observables, such as the forward-backward asymmetry A_{FB}. Unfortunately, this is beyond the scope of the present study.

Another interesting new direction would be the modification of the model underlying the numerical analysis. For example, one could consider a Z' coupled only to third generation fermions, as has been mentioned in the introduction (this would of course require one to analyze different data).

There are also several points in the study of dimuon production that could be amended to improve accuracy:

Experimental cuts[1] have already been mentioned. We take them into account insofar as we use the theoretical predictions given by most publications along with their experimental results, but to be consistent, one would have to apply the same cuts to the prediction including the Z'. Appearances to the contrary notwithstanding, this is a non-trivial task. While the experimental cuts are generally published, the data is sometimes already corrected to account for them, but this is not usually reported. Together with other corrections, this means that it is not obvious whether such a correction has already been done.

Radiative corrections are a somewhat similar case. These are higher-order corrections from QED, meaning that a photon may be emitted by an electron or muon, distorting the center-of-mass energy.

---

[1]Meaning that not all events are registered due to experimental limitations and analysis. The simplest example is a cut on the scattering angle imposed by the geometry of the detector; this is also the case we have treated in Section 1.3.3.

As with the experimental cuts, these corrections are incorporated in σ_{SM} (or so we assume) and thereby enter our analysis, but we neglect them for the Z′ contributions. It should be noted however that such corrections are most important near the Z′ resonance and negligible at far smaller energies.

Running coupling has been disregarded in this study. We treat α_{EM} as constant with the classical value of $\alpha_{\mathrm{EM}} \approx 1/137$.

The decay widths of the Z and Z′ also depend on the energy scale. We have treated them as constant.

QCD corrections to the width have also already been mentioned. See Section 1.4

For further information on the last four points, see [7] and references therein.

The ultimate analysis of the Z′ would take into account all available precision observables and perform a fit similar to those which have been done to obtain the values of the SM parameters. It is slightly inconsistent to use these parameters, that were fitted to a model without a Z′, in a model containing a Z′.

In spite of all these shortcomings, it is the opinion of this author that the results produced in the present study are meaningful and interesting in their own right.

Bibliography

[1] K. Abe *et al.* [VENUS Collaboration], Z. Phys. C **48** (1990) 13.

[2] R. Barate *et al.* [ALEPH Collaboration], Phys. Lett. B **399** (1997) 329.

[3] R. Barate *et al.* [ALEPH Collaboration], Eur. Phys. J. C **12** (2000) 183 [arXiv:hep-ex/9904011].

[4] W. Braunschweig *et al.* [TASSO Collaboration], Z. Phys. C **40** (1988) 163 [Erratum-ibid. C **42** (1989) 348].

[5] M. C. Gonzalez-Garcia and Y. Nir, Rev. Mod. Phys. **75** (2003) 345 [arXiv:hep-ph/0202058].

[6] F. Halzen, A. Martin, *Quarks and Leptons: An Introductory Course in Modern Particle Physics* (John Wiley & sons, New York, 1984)

[7] A. Leike, Phys. Rept. **317** (1999) 143 [arXiv:hep-ph/9805494].

[8] M. Jamin and M. E. Lautenbacher, Comput. Phys. Commun. **74** (1993) 265.

[9] S. Schael *et al.* [ALEPH Collaboration], Eur. Phys. J. C **49** (2007) 411 [arXiv:hep-ex/0609051].

[10] W. M. Yao *et al.* [Particle Data Group], J. Phys. G **33** (2006) 1.

[11] V. V. Nesvizhevsky, G. Pignol and K. V. Protasov, arXiv:0705.4478 [nucl-ex].

Appendix A

Experimental Data

Table A.1: Collected cross section data from various experiments, as used in the numerical analysis. Where the sources give separate statistical and systematic errors, we give the sum in quadrature. σ_{SM} is the theoretical prediction given by the source, if present.

$\sqrt{s}$ [GeV]	$\sigma_{\mu\mu}$ [pb]		σ_{SM} [pb]
TASSO@PETRA@DESY [4]			
13.9	472.7	$\pm$ 36	
22.3	184.7	$\pm$ 15.7	
34.5	73.2	$\pm$ 3	
35	66.1	$\pm$ 3.4	
38.3	56.4	$\pm$ 5.7	
43.6	42	$\pm$ 3	
VENUS@TRISTAN@KEK [1]			
50	62	$\pm$ 13.9	35.5
52	35.8	$\pm$ 4.8	33.0
55	31.2	$\pm$ 4.9	29.8
56	29.4	$\pm$ 3.3	28.9
56.5	29.6	$\pm$ 7.9	28.5
57	27.4	$\pm$ 3.8	28.0
58.3	29.9	$\pm$ 5.8	27.0
59.06	17.4	$\pm$ 4.4	26.5
60	24	$\pm$ 3.6	25.8
60.8	23.1	$\pm$ 3.1	25.3
ALEPH@LEP@CERN [2]			
63.12	25.3	$\pm$ 8.5	27.8
72.18	26.3	$\pm$ 3.7	26.3
78.29	32.5	$\pm$ 4.8	33
82.5	52	$\pm$ 5.3	52.5

Continued on next page

22

| $\sqrt{s}$ [GeV]	$\sigma_{\mu\mu}$ [pb]	σ_{SM} [pb]
85.2	95.6 ± 6.1	93.4
87.49	219 ± 10	211.8
88.37	336 ± 22	334.1
89.42	675.9 ± 7.5	671
90.21	1276 ± 44	1248.7
91.23	2001.8 ± 6	1991.1
92.05	1322 ± 40	1340.3
92.99	657 ± 6.8	649.8
94.03	381 ± 18	346.6
110.46	19 ± 10	17.5
130.2	10.2 ± 2.8	8.3
136.21	10.4 ± 2.6	7.2
ALEPH@LEP@CERN [3]		
130	7.9 ± 1.22	7
136	6.9 ± 1.12	6.1
161	4.49 ± 0.7	3.9
172	2.64 ± 0.54	3.3
183	2.98 ± 0.25	2.9
ALEPH@LEP@CERN [9]		
189	2.88 ± 0.14	2.83
192	2.86 ± 0.33	2.73
196	2.7 ± 0.19	2.61
200	2.99 ± 0.2	2.5
202	2.64 ± 0.26	2.44
205	1.92 ± 0.16	2.36
207	2.46 ± 0.15	2.32
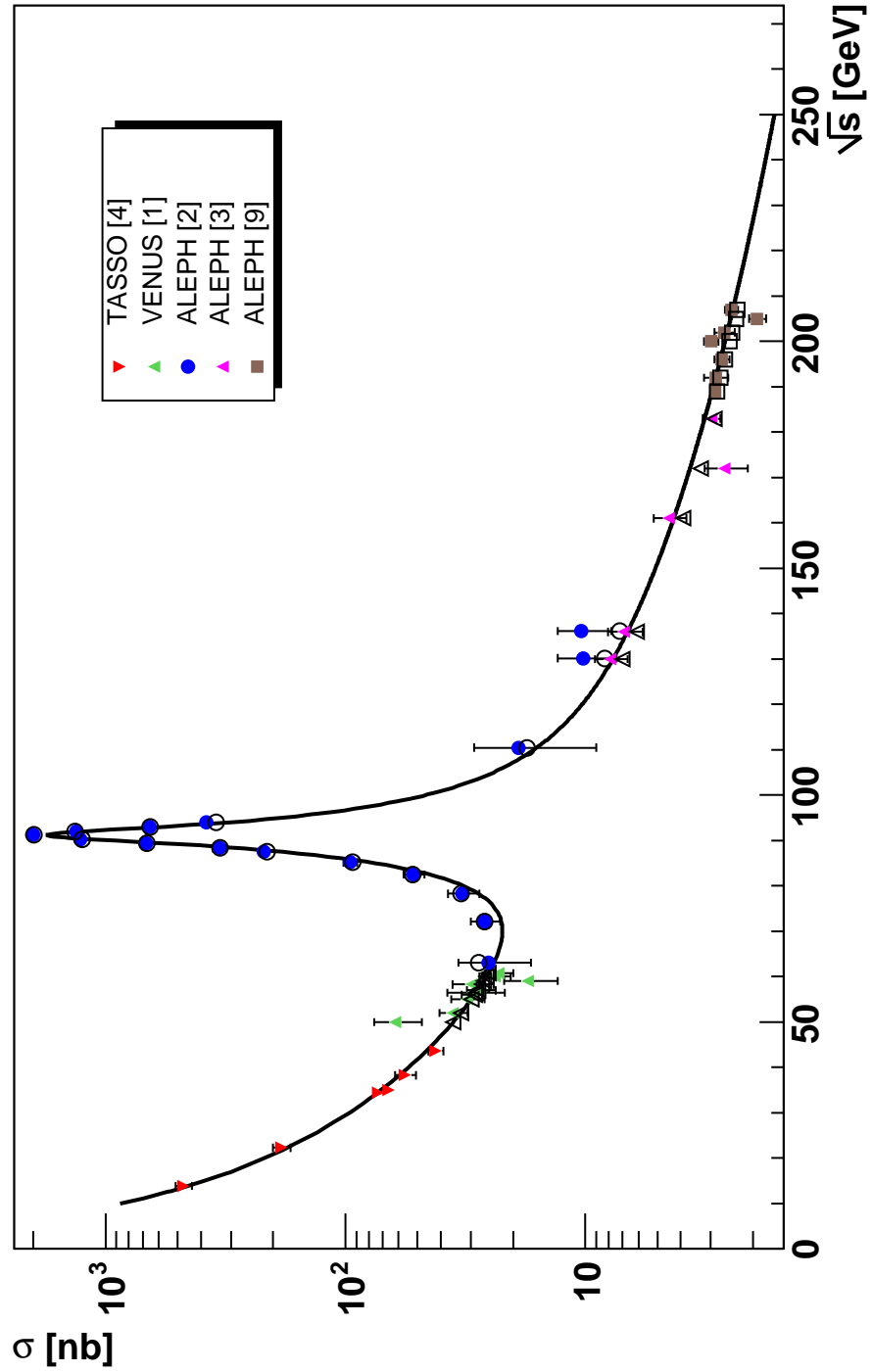
Figure A.1: The total integrated cross section of $e^-e^+ \to \mu^-\mu^+$. The solid black line is the SM prediction according to (1.23); the colored filled markers are the data points from Table A.1, the black open markers are the theory predictions given therein.

Appendix B

Computation of $\overline{\mathfrak{M}_B\mathfrak{M}^*_{B'}}$

In this appendix, we show how the BB' contribution to the squared martix element can easily be accomplished with the *Mathematica* program and the *Tracer* extension [8].

The following definitions represent those of Section 1.1:

```
1   (* We need TRACER *)
    <<"tracer.m"

3
    (* Some preliminary declarations *)
5   Clear[ka, la, mu, nu, s];
    VectorDimension[4];
7   AntiCommute[on];
    Spur[ls];

9
    (* Kinematic constraints.  We neglect lepton masses. *)
11  OnShell[on, {p1, 0}, {q1, 0}, {p2, 0}, {q2, 0},
                {p1, q1, s/2}, {p2, q2, s/2},
13              {p1, p2, -t/2}, {q1, q2, -t/2},
                {q1, p2, (s + t)/2}, {p1, q2, (s + t)/2}];

15
    chi[v_, k_] := (k.k - mass[v]^2 + I mass[v] width[v])^-1;
17  chiStar[v_, k_] := chi[v, k] /. I->(-I);

19  vertex[v_, f_, idx_] :=
      coupl[v] G[l, {idx}, vect[v, f] U - axial[v, f] G5];

21
    propagator[v_, k_, idx1_, idx2_] :=
23    {idx1}.{idx2} - k.{idx1}*k.{idx2}*propQFact[v]^2;

25  Ltens[v1_, v2_, f_, pa_, pb_, idx1_, idx2_] :=
      G[l, pa] ** vertex[v1, f, idx1] **
27    G[l, pb] ** vertex[v2, f, idx2]/2 /. l->ls;
```

```
29   MMstar [ v1_ ,  v2_ ,  k_ ]  :=
        chi [ v1 ,  k ]  chiStar [ v2 ,  k ]  *
31      Ltens [ v1 ,  v2 ,  electron ,  p1 ,  q1 ,  ka ,  la ]  *
        Ltens [ v2 ,  v1 ,  fermion ,  p2 ,  q2 ,  nu ,  mu ]  *
33      propagator [ v1 ,  k ,  ka ,  mu ]  *
        propagator [ v2 ,  k ,  la ,  nu ]  // ContractEpsGamma //  Simplify ;
```

Mathematica will now compute the desired result:

```
    In [2]:=  MMstar [B ,  B' ,  p1 + q1]  /.  t -> −s / 2  (1 −  Cos [ theta ])
 2  Out [2]=  (*  ...  *)
    In [3]:=  Ctens [ v1_ ,  v2_ ,  f1_ ,  f2_ ]  :=
 4      vect [ v1 ,  f1 ]  vect [ v1 ,  f2 ]  axial [ v2 ,  f1 ]  axial [ v2 ,  f2 ]  +
        vect [ v1 ,  f1 ]  axial [ v1 ,  f2 ]  axial [ v2 ,  f1 ]  vect [ v2 ,  f2 ]  +
 6      axial [ v1 ,  f1 ]  vect [ v1 ,  f2 ]  vect [ v2 ,  f1 ]  axial [ v2 ,  f2 ]  +
        axial [ v1 ,  f1 ]  axial [ v1 ,  f2 ]  vect [ v2 ,  f1 ]  vect [ v2 ,  f2 ];
 8  In [4]:=  Dtens [ v1_ ,  v2_ ,  f1_ ,  f2_ ]  :=
        vect [ v1 ,  f1 ]  vect [ v1 ,  f2 ]  vect [ v2 ,  f1 ]  vect [ v2 ,  f2 ]  +
10      vect [ v1 ,  f1 ]  axial [ v1 ,  f2 ]  vect [ v2 ,  f1 ]  axial [ v2 ,  f2 ]  +
        axial [ v1 ,  f1 ]  vect [ v1 ,  f2 ]  axial [ v2 ,  f1 ]  vect [ v2 ,  f2 ]  +
12      axial [ v1 ,  f1 ]  axial [ v1 ,  f2 ]  axial [ v2 ,  f1 ]  axial [ v2 ,  f2 ];
    In [5]:=  Out [2]  ==
14      s ^ 2  chi [B ,  p1+q1]  chiStar [B' ,  p1+q1]
        coupl [B] ^ 2  coupl [B'] ^ 2
16      (2  Ctens [B ,  B' ,  electron ,  fermion]  Cos [ theta ]  +
            Dtens [B ,  B' ,  electron ,  fermion]  (1 +  Cos [ theta ] ^ 2))
18          //  FullSimplify
    Out [5]=  True
```